RESEARCH ARTICLE

Impact of three decades of warming, increased nutrient availability, and increased cloudiness on the fluxes of greenhouse gases and biogenic volatile organic compounds in a subarctic tundra heath

Flobert A. Ndah[1] | Anders Michelsen[2] | Riikka Rinnan[2,3] | Marja Maljanen[1] | Santtu Mikkonen[1,4] | Minna Kivimäenpää[5]

[1]Department of Environmental and Biological Sciences, University of Eastern Finland, Kuopio, Finland

[2]Terrestrial Ecology Section, Department of Biology, University of Copenhagen, Copenhagen Ø, Denmark

[3]Department of Biology, Center for Volatile Interactions (VOLT), University of Copenhagen, Copenhagen Ø, Denmark

[4]Department of Technical Physics, University of Eastern Finland, Kuopio, Finland

[5]Natural Resources Institute Finland, Suonenjoki, Finland

Correspondence
Flobert A. Ndah, Department of Environmental and Biological Sciences, University of Eastern Finland, P.O Box 1627, 70211 Kuopio, Finland.
Email: flobert.ndah@uef.fi

Funding information
Finnish Cultural Foundation; Academy of Finland, Grant/Award Number: 348571 and 352968

Abstract

Climate change is exposing subarctic ecosystems to higher temperatures, increased nutrient availability, and increasing cloud cover. In this study, we assessed how these factors affect the fluxes of greenhouse gases (GHGs) (i.e., methane (CH_4), nitrous oxide (N_2O), and carbon dioxide (CO_2)), and biogenic volatile organic compounds (BVOCs) in a subarctic mesic heath subjected to 34 years of climate change related manipulations of temperature, nutrient availability, and light. GHGs were sampled from static chambers and gases analyzed with gas chromatograph. BVOCs were measured using the push-pull method and gases analyzed with chromatography–mass spectrometry. The soil temperature and moisture content in the warmed and shaded plots did not differ significantly from that in the controls during GHG and BVOC measurements. Also, the enclosure temperatures during BVOC measurements in the warmed and shaded plots did not differ significantly from temperatures in the controls. Hence, this allowed for assessment of long-term effects of the climate treatment manipulations without interference of temperature and moisture differences at the time of measurements. Warming enhanced CH_4 uptake and the emissions of CO_2, N_2O, and isoprene. Increased nutrient availability increased the emissions of CO_2 and N_2O but caused no significant changes in the fluxes of CH_4 and BVOCs. Shading (simulating increased cloudiness) enhanced CH_4 uptake but caused no significant changes in the fluxes of other gases compared to the controls. The results show that climate warming and increased cloudiness will enhance CH_4 sink strength of subarctic mesic heath ecosystems, providing negative climate feedback, while climate warming and enhanced nutrient availability will provide positive climate feedback through increased emissions of CO_2 and N_2O. Climate warming will also indirectly, through vegetation changes, increase the amount of carbon lost as isoprene from subarctic ecosystems.

KEYWORDS
biogenic volatile organic compounds, carbon and nitrogen cycling, cloud cover, greenhouse gases, nutrients, temperature, tundra

1 | INTRODUCTION

Northern high-latitude ecosystems are characterized by high soil organic carbon (C) (McGuire et al., 2009) and low nutrient availability due to cold temperatures that slow down organic matter decomposition and mineralization rates (Hobbie, 1996). Increased atmospheric concentrations of greenhouse gases (GHGs) from anthropogenic sources is changing the global climate (IPCC, 2021). Warming trends are projected to be stronger in the Arctic and Subarctic regions (IPCC, 2021; Rantanen et al., 2022), affecting (sub)arctic ecosystem structure and function. High temperatures accelerate the decomposition and mineralization of organic matter and thus stimulate nutrient availability (Hobbie et al., 2002; Mack et al., 2004; Rustad et al., 2001). In addition, increased moisture content and aerosol particles in a warmer atmosphere enhance cloud formation (Kecorius et al., 2019; Liu et al., 2012) and coupled with the projected increase in the poleward movement of clouds and maximum height of cloud formation (Norris et al., 2016), these cloud changes are predicted to substantially affect the surface energy balance in the Arctic and Subarctic. Clouds warm the Earth's surface by trapping and re-emitting longwave radiation and cool the surface by reflecting shortwave radiation that would otherwise be absorbed (Shupe & Intrieri, 2004). Clouds also reduce the amount of solar radiation reaching the Earth's surface (Kejna et al., 2021).

The changes in environmental conditions, that is, higher temperatures, increased nutrient availability, and increased cloudiness, are expected to affect a range of processes that control the ecosystem-atmosphere exchange of trace gases in northern high-latitude ecosystems. Carbon dioxide (CO_2) exchange in terrestrial ecosystems is mainly governed by photosynthesis and respiration (Trumbore, 2006) while the exchange of methane (CH_4) depends on the processes of methanogenesis and methanotrophy (Tate, 2015; Topp & Pattey, 1997; Whalen, 2005). The production of nitrous oxide (N_2O) in soil is mainly governed by nitrification and denitrification (Butterbach-Bahl et al., 2013). Biogenic volatile organic compounds (BVOCs) are atmospherically reactive gases and their emissions from plants and soils are usually linked to photosynthetic activity or enzymatic reactions and compound volatilization (Laothawornkitkul et al., 2009; Loreto & Schnitzler, 2010). The above-mentioned processes governing the gas fluxes and the magnitudes and directions of the fluxes are affected by increased temperature (Laothawornkitkul et al., 2009; Loreto & Schnitzler, 2010; Maes et al., 2024; Magnani et al., 2022; Tate, 2015; Topp & Pattey, 1997; Zhang et al., 2020), increased nutrient availability (Christensen et al., 1997; Gil et al., 2022; Mack et al., 2004; Tate, 2015; Valolahti et al., 2015; Wu et al., 2022), and reduced light (Christensen et al., 1997; Laothawornkitkul et al., 2009; Magnani et al., 2022). Higher temperatures, higher nutrient availability, and reduced light can also affect abiotic and biotic factors, such as soil temperature, soil moisture, substrate availability, microbial activity, and plant species composition, which in turn influence the gas fluxes (Ball et al., 2009; Gil et al., 2022; Hobbie et al., 2002; Jørgensen et al., 2015; Smith et al., 2000; Tate, 2015; Valolahti et al., 2015; Voigt et al., 2023; Zhang et al., 2020).

Quantifying the fluxes of GHGs and BVOCs in concert has significant implications in atmospheric chemistry. Increased atmospheric concentrations of CH_4, CO_2, N_2O, or BVOCs, due to enhanced plant productivity, substrate inputs, and decomposition and mineralization in a warmer climate, can trigger important climate feedback loops (IPCC, 2021; Kramshøj et al., 2019; Kulmala et al., 2014; McGuire et al., 2009; Schuur et al., 2008). Photo-oxidation of BVOCs by atmospheric oxidants can enhance the formation of secondary organic aerosols, which are precursors of cloud formation, thereby cooling the climate (Kulmala et al., 2014). Photo-oxidation of BVOCs can also extend the atmospheric lifetime of CH_4 by reducing the oxidative capacity of the atmosphere, contributing to positive feedback to climate (Bates & Jacob, 2019; Boy et al., 2022). In high-latitude trace gas studies, much attention has been directed towards peatland and wetland ecosystems, which are considered as significant atmospheric carbon sinks and sources of CH_4 (Emmerton et al., 2014; Frolking & Roulet, 2007). In recent years, it has become increasingly important to study sinks or sources of GHGs and BVOCs in different ecosystems including boreal forests, moist, mesic, and dry tundra or heath ecosystems and polar deserts (Emmerton et al., 2014; Hiltbrunner et al., 2012; Jørgensen et al., 2015; Michelsen et al., 2012; Siljanen et al., 2020; Wagner et al., 2019). However, to the best of our knowledge, studies investigating the fluxes of GHGs (i.e., CH_4, CO_2, N_2O) and BVOCs in concert in heath ecosystems spanning the Arctic and Subarctic tundra landscapes are lacking.

Since the impacts of climate change are expected to manifest over decades and centuries (Elmendorf et al., 2012), studies involving long term in situ field experiments are essential as they provide an opportunity to realistically simulate and study the effects of climate change (Elberling et al., 2008; Mastepanov et al., 2013; Natali et al., 2015; Pedersen et al., 2017) as well as verify observed responses after shorter time-spans and in laboratory conditions. Here, we present results of in situ CH_4, CO_2, N_2O, and BVOC flux measurements in a subarctic heath ecosystem in northern Sweden, which has been subjected to climate manipulations for over three decades. While a range of other ecosystem processes have been studied at this site previously (e.g., Christensen et al., 1997; Hicks et al., 2020; Illeris et al., 2004; Michelsen et al., 2012; Ravn et al., 2017; Rinnan et al., 2007), this study presents the first results on N_2O fluxes and measurements of GHGs and BVOCs in concert at the site. Our aim was to investigate the effects of long-term warming, increased nutrient availability, and shading (simulating increased cloudiness) on the fluxes of CH_4, CO_2 (i.e., total ecosystem respiration [ER]), N_2O, and BVOCs and to evaluate any relationships between the fluxes and plant species composition. Warming was expected to enhance CH_4 uptake due to increased soil temperature (Emmerton et al., 2014; Jørgensen et al., 2015) stimulating methanotrophic activity, and to increase ER (Pedersen et al., 2017; Ravn et al., 2017; Voigt, Lamprecht, et al., 2017) and N_2O emissions (Voigt, Lamprecht, et al., 2017; Zhang et al., 2020) due to increased C and nitrogen (N) turnover rates. Furthermore, warming was expected to increase emissions of the highly temperature dependent BVOCs (Li et al., 2023; Seco et al., 2022; Simin et al., 2021) as previously observed at

ecosystem-level (Faubert et al., 2010; Kramshøj et al., 2016; Tiiva et al., 2008; Valolahti et al., 2015). Fertilization was expected to decrease CH_4 uptake since N addition inhibits CH_4 consumption in natural upland ecosystems (Wu et al., 2022), and to increase ER (Christensen et al., 1997; Hicks et al., 2020) and N_2O emissions (Zhang et al., 2020) due to increased C and N turnover rates. Furthermore, fertilization was expected to increase BVOC emissions following enhanced vegetation growth and stimulation of microbial BVOC production under alleviated nutrient limitation (Valolahti et al., 2015). Shading was expected to decrease CH_4 uptake by decreasing soil temperature and methanotrophic activity and to decrease ER and N_2O emissions due to a decrease in C and N turnover rates (Christensen et al., 1997; Illeris et al., 2004). Moreover, shading was expected to decrease emissions of the light dependent BVOCs (Kramshøj et al., 2016; Laothawornkitkul et al., 2009).

2 | MATERIALS AND METHODS

2.1 | Study site and experimental design

The study was conducted in the growing season of 2022 (early to late July) in a heath tundra located just above the tree line (450m above sea level) near Abisko Scientific Research Station in northern Sweden (68°19′33.13″N, 18°51′13.09″E). The growing season in Abisko usually extends from June to September. The climate is subarctic with a mean annual air temperature of 0.5°C (30-year mean 1991–2020), and the warmest (July) and coldest (February) months have average temperatures of 12.2 and −9.8°C, respectively, and mean annual precipitation is 347mm (30-year mean 1991–2020) (Abisko Scientific Research Station, 2022). The vegetation at the site is characterized by a mixture of evergreen and deciduous dwarf shrubs, graminoids, forbs, mosses, and lichens, with *Cassiope tetragona* (L.) D. Don as the dominant plant species. The soil is characterized as a gelic gleysol and have formed on bedrock consisting mainly of base-rich mica schists. The organic soil horizon at the site is 12–20cm deep with a neutral pH (in H_2O) and approximately 90% soil organic matter in the top soil (Ravn et al., 2017; Rinnan et al., 2007; Ruess et al., 1999).

The field site is a long-term experimental site which was established in 1989 and has been maintained since then (Havström et al., 1993). The experiment mimics climate warming, increased nutrient availability, and increased cloudiness in a randomized block design. The experimental design has six treatments: control, warming, fertilization, shading, fertilization+warming and fertilization+shading (Rinnan et al., 2007). Each treatment is replicated in six blocks, yielding 36 plots (each $1.2 \times 1.2 m^2$) in total. In this study, we used four treatments: control, warming, fertilization, and shading, yielding a total of 24 plots. The warming treatment uses open top chambers (OTCs) made of 0.05mm transparent polyethylene film supported by dome-shaped PVC tubes (1989–2017), and 5mm polycarbonate plates forming a hexagonal OTC (2018 onwards) that were designed to increase air temperature by up to 3–4°C (Havström et al., 1993; Rieksta et al., 2021). The shading treatment uses dome-shaped hessian cloth tents that reduces incoming photosynthetic photon flux density (over the waveband 400–700nm) by 50%–60% (Ellebjerg et al., 2008). In the present study, the warming and shading treatments decreased photosynthetically active radiation (PAR) by 57% and 72%, respectively (Table 1). The warming and shading tents have been set up every year at the start of the growing season (~late May-early June) and removed at the end of the growing season (~late August-early September). Fertilization, mimicking the expected increase in soil nutrient availability due to atmospheric inputs and enhanced nutrient availability under a warmer climate (Rinnan et al., 2007), was provided by addition of $10 g m^{-2}$ NH_4NO_3–N, $2.6 g m^{-2}$ KH_2PO_4–P and $9 g m^{-2}$ KCl–K every June since 1990, except 1993 and 1998, and about half of this amount in 1989. The fertilization treatment had not significantly affected the soil pH (Hicks et al., 2020; Rinnan et al., 2007).

2.2 | Gas flux measurements and analyses

Fluxes of CH_4, CO_2 (ER) and N_2O were measured simultaneously in four campaigns, on July 7–8, July 13–14, July 18, and July 25–26. During measurements, a transparent polycarbonate chamber, $21 \times 21 \times 23$ cm, was placed on a metal frame base, 21.5×21.5 cm, which was preinstalled to a maximum depth of 5cm into the ground

TABLE 1 Chamber temperature (°C) and photosynthetically active radiation (PAR; µmol m^{-2} s^{-1}) during biogenic volatile organic compound (BVOC) measurements (mean ± SE, $n = 6$) in control (C), warming (W), and shading (S) plots/treatments in each measurement campaign and across measurement campaigns. Significant differences from control treatment in mean PAR during measurements in warming and shading treatments across campaigns are shown (Dunnett's test, *$p < .05$). Negative values indicate decreases.

	Chamber temperature (°C)			PAR (µmol m^{-2} s^{-1})		
	C	W	S	C	W	S
July 11–12	28.8 ± 2.2	28.1 ± 3.1	28.5 ± 2.8	1032 ± 164	466 ± 194	295 ± 26
July 19–20	19.6 ± 1.1	20.2 ± 1.5	18.6 ± 1.2	874 ± 167	336 ± 26	218 ± 41
July 28	14.1 ± 0.6	14.4 ± 0.6	13.9 ± 0.5	282 ± 69	134 ± 43	93 ± 28
Across campaigns	20.8 ± 1.7	20.9 ± 1.7	20.3 ± 1.8	729 ± 109	312 ± 71	202 ± 27
W and S effect (%)					−57*	−72*

in each plot. Using a water lock in the frame base, the chamber seals tight to the frame, thus creating gas-tight enclosure open only to the ground during measurements. The chamber was covered with an opaque plastic bag to create dark conditions. The air in the chamber headspace was circulated with a small fan during the measurement period. Gas samples (25 mL) taken from the chamber headspace with a syringe (60 mL) at time intervals of 0, 10, 20 and 60 min after enclosure of the chamber were injected into 12 mL pre-evacuated vials (Labco Exetainers®, UK). Gas samples were analyzed for CH_4, CO_2, and N_2O concentrations with a gas chromatograph (Agilent 7890B, Agilent Technologies, USA), equipped with an autosampler (Gilson GX—271, Gilson Inc, USA), with flame ionization detector (FID) for CH_4, thermal conductivity detector (TCD) for CO_2, and an electron capture detector (ECD) for N_2O. The detector temperatures were 250, 200, and 300°C for FID, TCD, and ECD, respectively, and the oven temperature was 60°C. Nitrogen (flow = 40 mL min^{-1}) was used as a carrier gas for FID and TCD, and helium (flow = 40 mL min^{-1}) for ECD. The sensitivity of the ECD was improved by adding a 5% CH_4/95% Ar gas mixture (flow = 2 mL min^{-1}) to the carrier gas flow. Compressed air containing 2.02 ppm CH_4, 398 ppm CO_2, and 0.836 ppm N_2O was used for calibration. The flux rates were calculated from the linear change (increase or decrease) in the gas concentrations in the chamber headspace using the equation:

$$\text{Flux} = \frac{k \times P \times V \times M}{R \times T \times A},$$

where $k = CH_4$, CO_2, or N_2O slope, P = pressure inside the chamber (kPa), V = volume of the chamber headspace (m^3), M = molar mass (g mol^{-1}) of respective gas, R = ideal gas constant (8.314 J k^{-1} mol^{-1}), T = chamber temperature (K) and A = base area (m^2). Fluxes are expressed as μg m^{-2} h^{-1} for CH_4 and N_2O and mg m^{-2} h^{-1} for CO_2. By convention, negative fluxes of CH_4 correspond to a net uptake of the GHG by the ecosystem.

BVOC emissions within the same installed frames as used for the GHG measurements were measured in 3 campaigns on July 11–12, July 19–20, and July 28 using a conventional push-pull system (Faubert et al., 2012; Tholl et al., 2006). Measurements were made with transparent polycarbonate chambers (thickness 1.5 mm, 220×220 mm, height 200 mm; Vink Finland, Kerava, Finland) placed on the installed frames. The collar grooves were filled with water before placing the chamber to create an airtight headspace inside the chamber. The chamber was flushed for 30 min with a flow rate of 300 mL min^{-1} to replace the headspace with filtered air (Ortega & Helmig, 2008) prior to the 30-min-long measurement. During the measurement, the air was circulated through the chambers using battery-operated pumps (12 V; Rietschle Thomas, Puchheim, Germany) at 300 mL min^{-1} for inflow and 200 mL min^{-1} for outflow. The chambers were equipped with fans to ensure well-mixed headspace. The incoming air was filtered for particles and background hydrocarbons and scrubbed for ozone in order to avoid losses of the highly reactive BVOCs (Valolahti et al., 2015). The BVOCs released from the plots were trapped in stainless steel adsorbent tubes (125 mg Tenax TA, 125 mg Carbopack B, Markes International Limited, Llantrisant, UK). After the collection, the tubes were sealed with Teflon-coated brass caps and stored at +4°C until analysis. Blank measurements were conducted to account for compounds derived from sampling materials and the analytical system. During blank measurements, the entire plot area within the installed metal frames were covered with pre-cleaned (120°C for 1 h) polyethylene terephthalate film and the collar grooves filled with water to create an airtight headspace inside the chamber. During the measurements, temperature and relative humidity inside the chamber enclosure (DS1923-F5, iButton Hygrochron temperature/humidity logger, Maxim Integrated Products Inc., CA, USA) and PAR (photosynthetic light smart sensor S-LIA-M003, connected to HOBO micro station data logger H21-002, Onset Computer Corporation, Bourne, MA, USA) were recorded every minute and every tenth second, respectively. See Table 1 for chamber temperature and PAR during measurements.

BVOC samples were analyzed using gas chromatography–mass spectrometry (Hewlett-Packard GC type 6890, Germany; MSD 5973, UK) after thermal desorption with automatic thermal desorber (Perkin-Elmer ATD400 Automatic Thermal Desorption system, Wellesley, MA, USA) at 250°C for 10 min and cryofocusing at −30°C. The carrier gas was helium with a constant flow rate of 1.2 mL min^{-1}. The oven temperature was held at 40°C for 2 min and then programmed to ramp to 210°C at a rate of 5°C min^{-1} and finally to 250°C at a rate of 20°C min^{-1}. An HP-5MS capillary column (model 19091S-436; 60 m×0.25 mm i.d (inner diameter)×0.25 μm film thickness; Agilent, Santa Clara, CA, USA) was used for the separation of BVOCs. Chromatograms were analyzed using the software PARADISe v. 6.0 (Quintanilla Casas et al., 2023). Compounds were identified using pure standards, when available, or tentatively identified using the NIST 2020 Mass Spectral Library (National Institute of Standards and Technology, Gaithersburg, MD, USA). For tentative identification, only compounds with a match factor >800 and probability >30 were considered for further analysis. BVOC concentrations were quantified using external standards. Compounds for which pure standards were unavailable were quantified using the closest structurally related standard compound (Table S1). Compounds that are known to arise from plastics, the analytical system, sorbent tubes, or personal care products were excluded from the dataset, including siloxanes, phthalates, dibutyl adipate, 2-ethylhexyl salicylate, and homosalate. Compounds smaller than isoprene were also excluded from the dataset because the adsorbent tubes cannot reliably trap lighter BVOCs. Compounds were categorized into the following groups: isoprene, non-oxygenated monoterpenes (nMTs), oxygenated monoterpenes (oMTs), sesquiterpenes (SQTs), and other BVOCs. BVOC concentrations in blanks were subtracted from those in the samples. BVOC emission rates were expressed on ground area basis (μg m^{-2} h^{-1}). The emission rates were also standardized to the temperature of 30°C and the PAR of 1000 μmol m^{-2} s^{-1} according to Guenther et al. (1993, 1995) to minimize the effects caused by variation in environmental conditions.

2.3 | Soil, weather, and climate data

During the gas flux measurements, soil temperature and moisture were measured manually in the experimental plots next to the chamber base. Soil temperature was taken at 5 cm depth using a portable single input K/J thermometer (TENMARS TM-80 N, Taiwan). Soil moisture was measured three times in each plot using a hand-held ML2x Theta Probe (Delta-T Devices Ltd., Cambridge, UK), and the averages were subsequently used. Additionally, continuous measurements of air temperature at the soil surface (referred to as surface temperature) and soil temperature at 3 cm depth were obtained from temperature loggers (Tiny Tags, TGP-4520, Gemini Data Loggers Ltd., Chichester, UK) that were placed in four warming and three control, shading, and fertilization plots throughout the growing season. Soil and surface temperatures were logged hourly. Meteorological data on air temperature, precipitation, and PAR were acquired from Abisko Scientific Research Station, including detailed hourly data from 1 June to 30 September 2022 (Abisko Scientific Research Station, 2022) and 30-year mean data for air temperature and precipitation from 1991 to 2020 (Abisko Scientific Research Station, 2022).

2.4 | Vegetation analyses

Vegetation cover and composition inside the installed metal frames in each plot were assessed on 6–7 July using the point intercept method with 49 intersects according to Jonasson (1988). All plants were identified to species level and grouped into the functional groups; evergreen shrubs, deciduous shrubs, graminoids, forbs, mosses, and lichens. The cover of litter within the installed metal frames was also assessed. In addition, normalized differential vegetation index (NDVI) was measured for each plot, using a SKR 110 sensor (Skye Instruments) with narrow band interference filters centered at 660 and 730 nm, to obtain an estimate of the greenness of each plot.

2.5 | Statistical analyses

Treatment effects on CH_4, CO_2 (ER), N_2O, and BVOC fluxes, and manual measurements of soil temperature and moisture across the study period were analyzed using linear mixed-model (LMM) analysis of variance (IBM SPSS Statistics 27.0.0, SPSS Inc. IBM Company ©, Armonk, NY, USA). The model included treatment (four levels: control, warming, fertilization, and shading) as a fixed factor, block and measurement campaign as random factors, and temperature at 5 cm depth and soil moisture as covariates. In addition, LMM were run separately for each campaign to evaluate treatment effects on the gas flux variables within each campaign with treatment (four levels: control, warming, fertilization, and shading) and block as factors. One-way ANOVA with Tukey's test was used to evaluate treatment effects on surface temperature and temperature at

3 cm soil depth during the sampling month and growing season. Dunnett's test was used to compare temperature and PAR during BVOC measurements in warming and shading treatments to the control. Treatment effects on vegetation variables (percentage cover of plant functional groups and NDVI) were assessed using similar LMM models as described earlier for analysis of the gas flux variables within each campaign. The Bonferroni test was used to examine differences between control, warming, fertilization, and shading, when the factor "treatment" was significant ($p < .05$) or marginally significant ($.05 < p < .1$). Data were tested for normality and homogeneity of variance using the Shapiro–Wilk's normality test and by evaluating residual plots and log-transformed, if necessary.

Principal component analysis (PCA) in SIMCA 17.0.2 (Umetrics, Umeå, Sweden) was used to evaluate the main effects of warming, fertilization, and shading on the percentage cover of individual plant species. PCA components were extracted using cross validation, centering, and unit-variance scaling of the variables (cover of individual plant species). The scores for the first two components were analyzed using similar LMM models as reported earlier for the vegetation data. Partial least squares (PLS) regression (SIMCA 17.0.2, Umetrics, Umeå, Sweden) was used to assess covariance between the gas fluxes (dependent variables, Y) and vegetation cover (percentage cover of individual plant species) (independent variables, X). The PLS analysis was performed for the gas flux measurement dates closest to the vegetation analysis. A separate model was fitted for each gas (y variable). In all PLS regression analyses, models were extracted following centering and unit variance scaling of the variables. The extracted models had one component and variables with VIP (Variable Influence on Projection) <.5 were excluded from the model. The significance of the models were tested using analysis of variance of the cross-validated residuals (CV-ANOVA, Eriksson et al., 2008).

3 | RESULTS

3.1 | Weather and soil properties

During the growing season, June, 1–September 30, 2022, hourly air temperature in Abisko ranged from −2.7 to 28.2°C with an average of $10.0 \pm 0.1°C$ while hourly PAR averaged $303.0 \pm 7.0 \mu mol\, m^{-2}\, s^{-1}$ reaching a maximum of $1679 \mu mol\, m^{-2}\, s^{-1}$. Peak hourly air temperature (28.2°C) and PAR ($1679 \mu mol\, m^{-2}\, s^{-1}$) occurred on 28 and 23 June, respectively. Total precipitation reached 192 mm with 35 days of rainfall (>1 mm). During the sampling month, 1 to 31 July 2022, hourly air temperature varied from 4.7 to 26.8°C, averaging $12.0 \pm 0.1°C$, representing the warmest month of the growing season, and precipitation totaled 93 mm across 8 days of rainfall (>1 mm). Air temperature, precipitation, and PAR (June to September 2022) in Abisko, and surface temperature and temperature at 3 cm soil depth (June to August 2022) at measurement field site are presented in Figure 1.
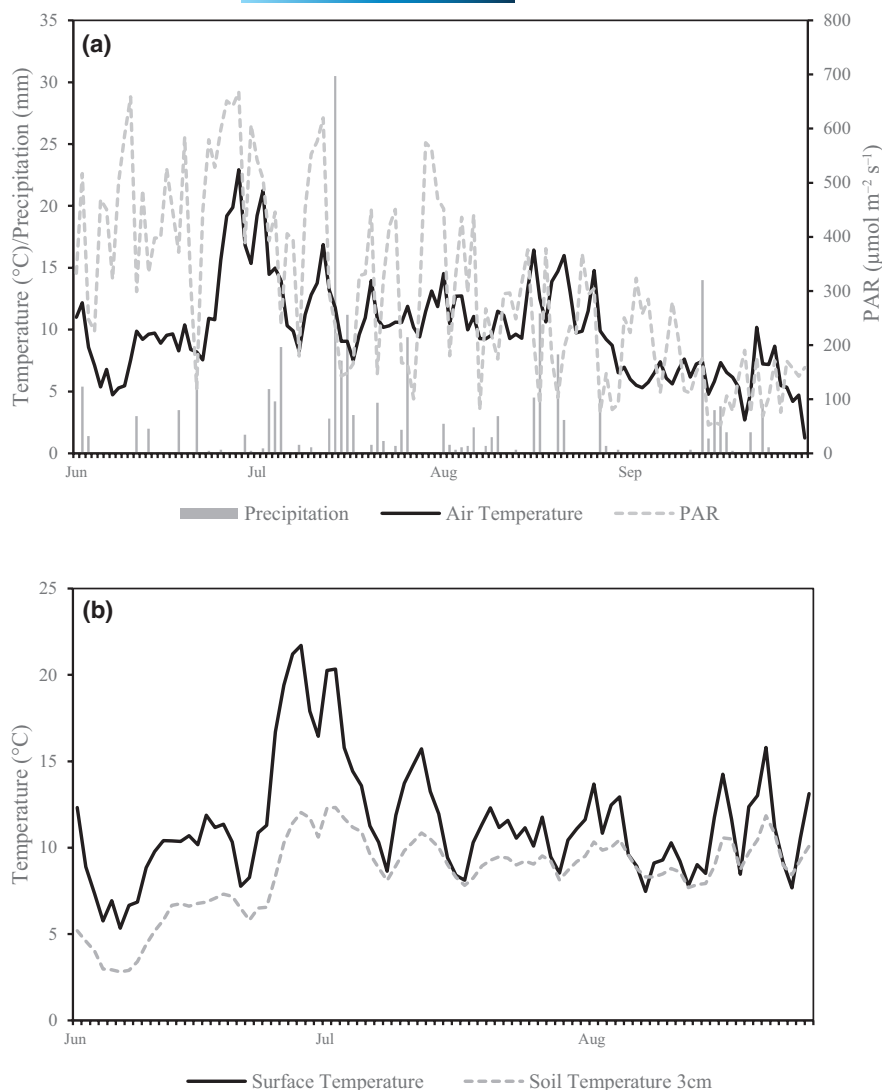
FIGURE 1 (a) Daily precipitation and mean daily air temperature and photosynthetically active radiation (PAR) in Abisko (1 June to 30 September; Abisko Scientific Research Station) and (b) mean daily surface and soil (3 cm depth) temperature in control plots at measurement field site ($n=3$; 2 June to 26 August) in the growing season 2022.

There were no significant treatment effects on the surface temperature during the sampling month (July 2022) or growing season (June to August 2022) (Table 2). Similarly, soil temperature at 3 cm depth was not significantly affected by the treatments, except that the shading plots tended to have a lower soil temperature at 3 cm depth compared to the warming plots (Table 2). Across all campaigns, during the GHG and BVOC measurements, soil moisture (manual measurements) was significantly lower in the fertilization treatment compared to the control while there were no significant treatment effects on soil temperature at 5 cm depth during flux measurements (Table 3).

3.2 | Ecosystem gas fluxes

Across all measurement campaigns, CH_4 fluxes ranged from 1.7 to $-107.4\,\mu g\,m^{-2}\,h^{-1}$ among all plots and from -3.7 to $-63.5\,\mu g\,m^{-2}\,h^{-1}$ in control plots only. A total of 98% of all fluxes were negative,

	C	W	F	S	*p*-Value
Sampling month (1–31 July 2022)					
Surface temperature	12.0 ± 0.3	12.7 ± 0.2	12.5 ± 0.1	12.7 ± 0.1	.172
Soil temperature at 3 cm depth	9.6 ± 0.6	10.0 ± 0.4	9.5 ± 0.6	8.2 ± 0.1	.082
Growing season (2 June–26 August 2022)					
Surface temperature	11.4 ± 0.4	12.2 ± 0.2	11.8 ± 0.2	11.9 ± 0.2	.153
Soil temperature at 3 cm depth	8.5 ± 0.5	8.9 ± 0.4	8.4 ± 0.6	7.1 ± 0.2	.086

TABLE 2 Surface temperature and soil temperature at 3 cm depth from continuous measurements averaged across the sampling month and growing season (mean ± SE) in control (C) ($n=3$), warming (W) ($n=4$), fertilization (F) ($n=3$), and shading (S) ($n=3$) plots.

TABLE 3 Manual measurements of soil temperature at 5 cm depth and soil moisture during gas flux measurements averaged in each measurement campaign and across measurement campaigns (mean ± SE, $n=6$) in control (C), warming (W), fertilization (F), and shading (S) plots. p-values from linear mixed-model for main effects of treatment (T) across measurement campaigns are shown and $p < .05$ emboldened. Treatments not sharing a superscript letter across measurement campaigns differ significantly from each other.

|	C	W	F	S	p-Value T
GHG measurements					
Soil temperature 5 cm					
July 7–8	8.6 ± 1.0	9.7 ± 1.2	8.4 ± 0.5	7.6 ± 0.4	
July 13–14	10.6 ± 0.8	10.3 ± 0.5	10.4 ± 0.6	9.9 ± 0.5	
July 18	9.5 ± 1.0	9.3 ± 0.8	9.3 ± 0.5	8.7 ± 0.5	
July 25–26	9.2 ± 0.4	8.8 ± 0.6	9.1 ± 0.3	8.6 ± 0.3	
Across campaigns	9.5 ± 0.4	9.5 ± 0.4	9.3 ± 0.3	8.7 ± 0.3	.176
Soil moisture					
July 7–8	23.0 ± 1.9	20.7 ± 1.4	15.3 ± 3.5	19.7 ± 1.6	
July 13–14	23.0 ± 0.9	18.7 ± 3.3	12.9 ± 1.0	18.7 ± 3.9	
July 18	28.7 ± 2.5	26.3 ± 2.3	24.6 ± 2.2	29.0 ± 4.2	
July 25–26	26.1 ± 2.1	19.0 ± 1.2	20.7 ± 1.4	24.0 ± 4.4	
Across campaigns	25.2 ± 1.0[a]	21.2 ± 1.2[ab]	18.4 ± 1.4[b]	22.9 ± 1.9[ab]	**.002**
Biogenic volatile organic compound measurements					
Soil temperature 5 cm					
July 11–12	11.2 ± 0.5	13.3 ± 0.6	12.0 ± 0.6	12.8 ± 0.6	
July 19–20	10.0 ± 0.6	10.3 ± 0.9	11.5 ± 0.7	10.5 ± 0.6	
July 28	7.6 ± 0.4	7.4 ± 0.2	7.4 ± 0.2	7.1 ± 0.2	
Across campaigns	9.6 ± 0.4	10.3 ± 0.7	10.3 ± 0.6	10.1 ± 0.6	.210
Soil moisture					
July 11–12	20.2 ± 1.3	20.2 ± 3.5	14.3 ± 0.5	19.1 ± 2.4	
July 19–20	29.9 ± 2.7	23.7 ± 1.7	20.7 ± 1.5	25.2 ± 2.0	
July 28	26.1 ± 1.9	25.1 ± 2.9	22.4 ± 1.4	21.7 ± 2.1	
Across campaigns	25.4 ± 1.5[a]	23.0 ± 1.6[ab]	19.1 ± 1.1[b]	22.0 ± 1.3[ab]	**.003**

indicating primarily CH_4 uptake. The warming treatment increased CH_4 uptake by 81% and 66% compared to the control and fertilization treatments, respectively (Figure 2A). The shading treatment also increased CH_4 uptake by 96% and 79% compared to the control and fertilization treatments, respectively (Figure 2A). When the measurement campaigns were analyzed separately, the effects of warming and shading were significant on July 7–8, July 13–14, and July 18 measurement campaigns (Figure 2A).

Across all measurement campaigns in control plots, ER varied from 23.3 to 787.4 mg m^{-2} h^{-1} and averaged 313.9 ± 43.1 mg m^{-2} h^{-1}. The warming treatment increased ER by 64% and 150% compared to the control and shading treatments, respectively (Figure 2B). The fertilization treatment increased ER by 98% and 202% compared to the control and shading treatments, respectively (Figure 2B). The effects were significant in all campaigns and were most pronounced on July 18 measurement campaign (Figure 2B).

The fluxes of N_2O ranged from 0.2 to 19.6 µg m^{-2} h^{-1} among all plots and from 0.2 to 2.6 µg m^{-2} h^{-1} in control plots only across all measurement campaigns. The warming and fertilization treatments increased N_2O emissions, eight and twentyfold respectively, compared

to the control (Figure 2C). Fertilization also increased N_2O emissions sevenfold compared to shading (Figure 2C). The effects were significant on July 7–8, July 18, and July 25–26 measurement campaigns (Figure 2C).

Across all treatments and measurement campaigns, BVOC emissions comprised of isoprene, MTs (nMTs and oMTs), SQTs, and other BVOCs contributing 7%, 27%, 35%, and 30% respectively of the total BVOC emissions (Figure S1). Emission rates of individual BVOCs are shown in Tables S2–S4. Total BVOC emissions averaged 112.9 ± 77.0 µg m^{-2} h^{-1} in control plots across all measurement campaigns. The most dominant MT was eucalyptol while α-eudesmol was the most dominant SQT. The MTs α-pinene and linalool as well as SQTs α-copaene and γ-eudesmol were also emitted in significant amounts. Warming increased isoprene emission rates ninefold compared to the shading treatment and the effect was significant on July 19–20 measurement campaign (Figure 3A). Warming increased standardized isoprene emissions five and eightfold compared to the control and shading treatments, respectively and the effect was significant on July 19–20 measurement campaign (Figure 3B). There were no significant treatment effects on the emission rates
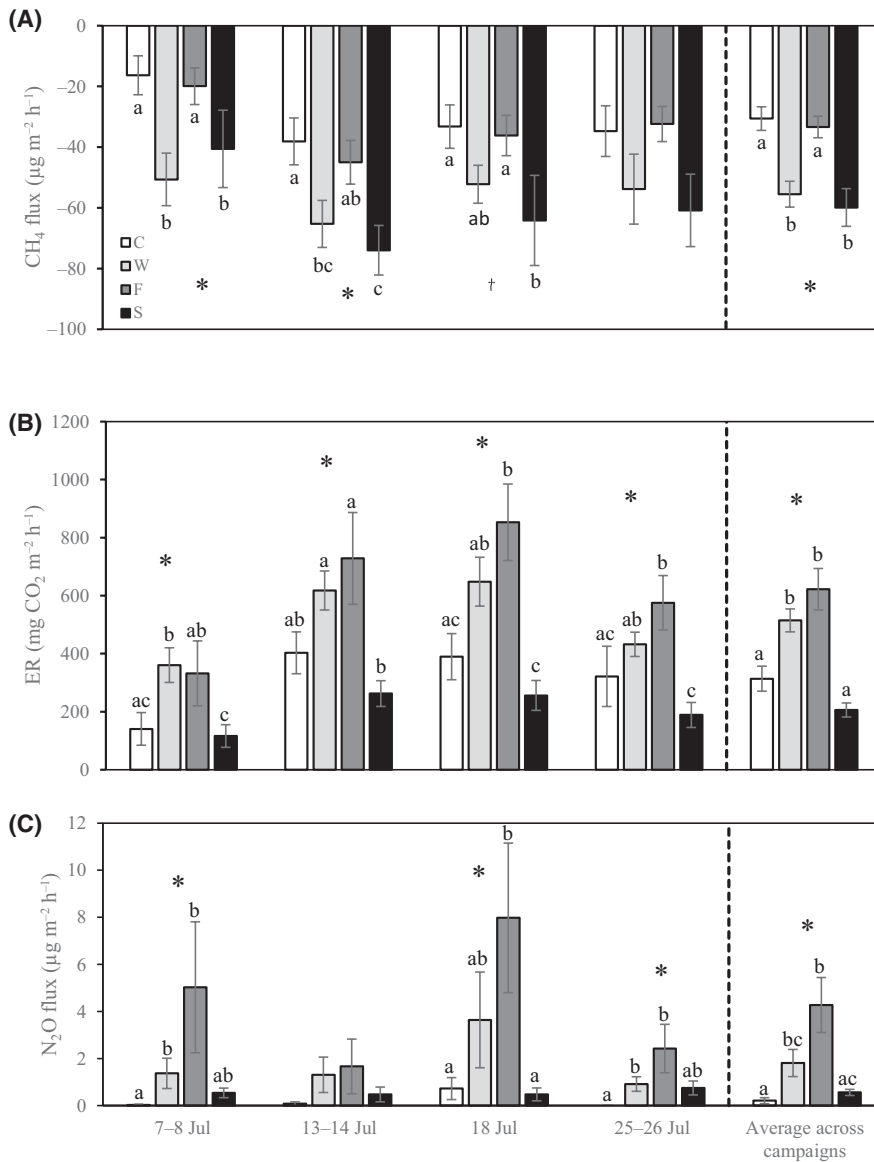
FIGURE 2 Fluxes of (A) CH_4, (B) CO_2, and (C) N_2O for each measurement campaign and averaged across measurement campaigns ($\pm$ SE, $n = 6$) in control (C), warming (W), fertilization (F), and shading (S) plots. Significant ($p < .05$) and marginally significant ($.05 < p < .1$) effects of treatment for linear mixed-model (LMM) are indicated by * and †, respectively. Treatments not sharing a letter within a measurement campaign and across measurement campaigns differ significantly from each other ($p < .05$, LMM with Bonferroni test). ER, ecosystem respiration.

or standardized emissions of the other BVOC groups (Table S5). Soil temperature and moisture during measurements had no significant effects on any of the gas fluxes ($p > .05$).

3.3 | Vegetation cover and greenness

In general, the dominant plant functional group was evergreen shrubs followed by deciduous shrubs (Table 4). The most dominant evergreen shrubs were *Empetrum hermaphroditum* and *C. tetragona* while the deciduous shrubs were dominated by *Betula nana* and *Vaccinium uliginosum*. The graminoids present in the plots were mainly *Carex vaginata* and *Poa alpigena*. Mosses were dominated by *Hylocomium splendens*.

The fertilization treatment increased the cover of graminoids compared to the control, warming, and shading treatments and increased the total vascular plant cover compared to the control and shading treatments (Table 4). The increase in graminoid cover was

mainly due to changes in *P. alpigena* (Table 4; Figure 4). The percentage cover of *P. alpigena* was higher in the fertilization treatment compared to the control and shading treatments as was detected along PC1 (Figure 4). Mosses and lichens were absent in the fertilized but not in the control, warmed, and shaded plots (Table 4; Figure 4). The cover of litter was significantly increased by the warming and fertilization treatments compared to the control (Table 4). The warming treatment also increased the cover of litter compared to shading (Table 4). A positive correlation was found between the abundance of *C. vaginata*, *Cladonia* sp., *H. splendens*, and *Astragalus alpinus*, as well as between the abundance of *Salix reticulata*, *Cetraria nivalis*, *Equisetum scirpoides*, other lichens, and *C. tetragona* (Figure 4). The abundance of these species was negatively correlated with that of *E. hermaphroditum* and *P. alpigena* (Figure 4).

The shading treatment decreased NDVI compared to the control and warming treatments (Figure 5). The fertilization treatment also showed lower NDVI compared to the warming treatment (Figure 5).

FIGURE 3 (A) Emission rates and (B) standardized emissions of isoprene for each measurement campaign and averaged across measurement campaigns ($\pm$SE, $n=6$) in control (C), warming (W), fertilization (F), and shading (S) plots. Significant ($p<.05$) and marginally significant ($.05<p<.1$) effects of treatment for linear mixed-model (LMM) are indicated by * and $\dagger$, respectively. Treatments not sharing a letter within a measurement campaign and across measurement campaigns differ significantly from each other ($p<.05$, LMM with Bonferroni test).
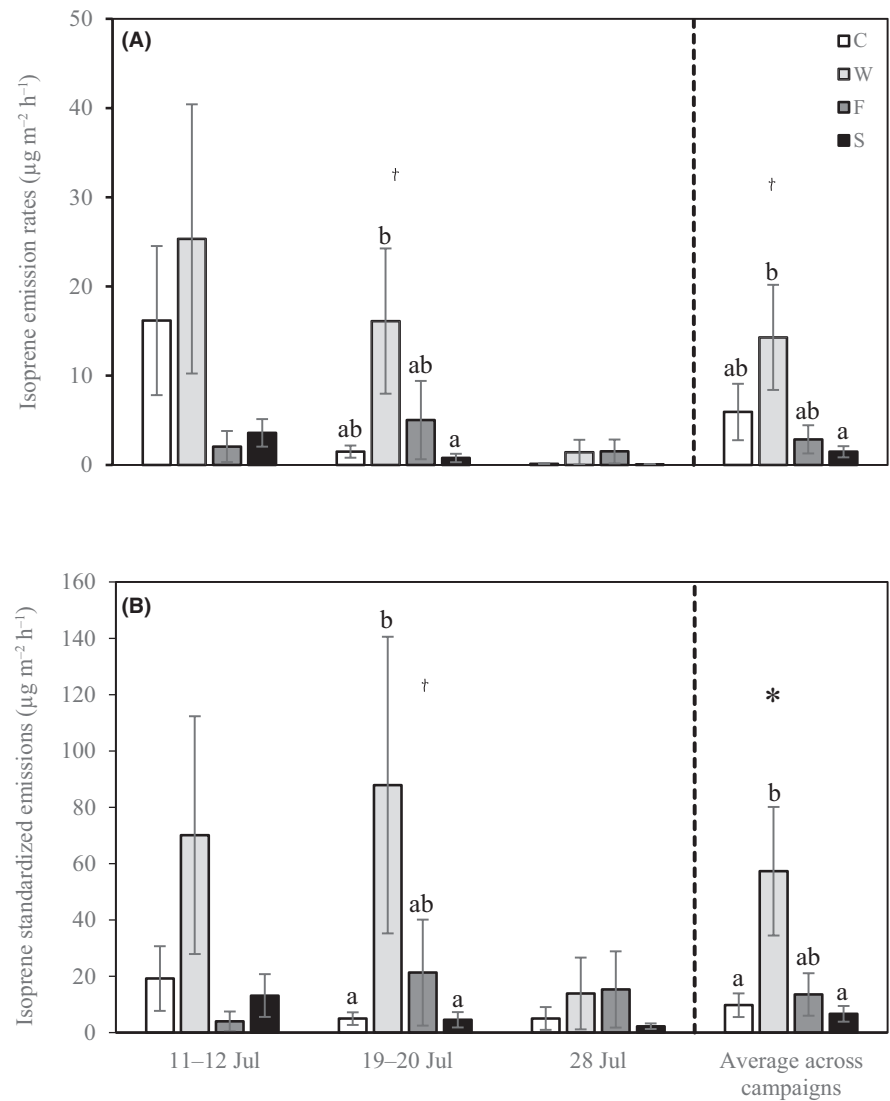
3.4 | Covariance between gas flux and vegetation

According to the PLS regression, isoprene was negatively associated with the cover of *E. hermaphroditum* and *P. alpigena* and positively with the cover of *V. uliginosum*, *E. scirpoides*, and *H. splendens* (Figure 6).

4 | DISCUSSION

This study demonstrates that more than 30 years of warming and nutrient addition at a subarctic mesic heath have led to increased CO_2 and N_2O emissions. We also observed enhanced CH_4 uptake in response to warming and shading, and increased isoprene emissions in response to warming at the site. The study is the first to show impact of more than three decades of warming, increased nutrient availability, or shading on GHG and BVOC fluxes in subarctic tundra. The observed responses were likely due to both current environmental conditions and accumulated long-term effects of the climate treatment manipulations on soil properties and vegetation. This

highlights the importance of long-term climate manipulation experiments in predicting the outcome and likelihood of ecosystem driven climate feedbacks (Michelsen et al., 2012).

4.1 | Ecosystem respiration

The rates of CO_2 efflux were of the same order of magnitude as earlier flux measurements at the site (Christensen et al., 1997; Hicks et al., 2020; Ravn et al., 2017) and at a nearby wet heath (Pedersen et al., 2017). In line with our expectations, the warming and fertilization treatments increased CO_2 emissions from the heath. Our results correspond with previous findings of warming-induced increase in ER after 22 years of warming (Ravn et al., 2017) and fertilization-induced increase in ER after 22 years (Ravn et al., 2017) and 26 years (Hicks et al., 2020) of nutrient addition at the same site. Together, these findings suggest that the effects of warming and increased nutrient availability are not weakening through time (Maes et al., 2024; Ravn et al., 2017). The effects of warming and increased nutrient availability on surface temperature and soil temperature at 3 and

TABLE 4 Vegetation cover (%, mean ± SE, $n = 6$) of plant species in control (C), warming (W), fertilization (F) and shading (S) plots/treatments in July 2022.

					p-Value
	C	W	F	S	T
Plant species functional group					
Evergreen shrubs	45.2 ± 9.9	40.5 ± 15.5	83.3 ± 14.1	45.2 ± 6.5	.199
Deciduous shrubs	22.1 ± 7.4	62.6 ± 19.1	19.4 ± 6.3	11.6 ± 4.8	.382
Graminoids	4.8 ± 1.1[a]	11.9 ± 7.3[a]	48.6 ± 9.7[b]	7.8 ± 3.6[a]	**<.001**
Forbs + vascular cryptograms	22.8 ± 9.1	11.2 ± 5.9	7.8 ± 3.2	17.0 ± 7.8	.259
Total vascular plants	94.9 ± 14.1[a]	126.2 ± 9.3[ab]	159.2 ± 21.2[b]	81.6 ± 3.7[a]	**.005**
Mosses	22.8 ± 7.0[a]	8.5 ± 6.4[ab]	0.0[b]	10.2 ± 3.5[ab]	**.009**
Lichens	4.4 ± 1.8[a]	1.0 ± 1.0[ab]	0.0[b]	4.4 ± 2.9[ab]	**.014**
Litter	28.9 ± 5.4[a]	62.9 ± 7.4[b]	52.7 ± 6.5[bc]	31.0 ± 2.9[ac]	**<.001**
Plant species					
Evergreen shrubs					
Andromeda polifolia	2.0 ± 1.3	1.4 ± 1.4	0.0	0.0	-
Cassiope tetragona	31.0 ± 10.5	9.9 ± 5.1	14.6 ± 6.3	15.0 ± 6.5	-
Dryas octopetala	0.3 ± 0.3	0.3 ± 0.3	0.0	0.0	-
Empetrum hermaphroditum	7.5 ± 5.7	27.6 ± 17.8	59.9 ± 15.8	18.4 ± 6.6	-
Rhododendron lapponicum	0.7 ± 0.7	0.7 ± 0.7	1.0 ± 1.0	4.4 ± 2.9	-
Vaccinium vitis-idaea	3.7 ± 3.7	0.4 ± 0.4	7.8 ± 5.7	7.5 ± 7.5	-
Deciduous shrubs					
Arctostaphylos alpinus	1.4 ± 1.4	11.6 ± 11.6	0.0	4.4 ± 4.0	-
Betula nana	11.2 ± 7.0	31.3 ± 20.0	1.0 ± 1.0	2.7 ± 2.7	-
Salix hastata	0.0	0.0	7.5 ± 4.3	0.7 ± 0.7	-
Salix myrsinites	0.3 ± 0.3	2.7 ± 2.7	0.7 ± 0.7	0.0	-
Salix reticulata	2.7 ± 2.0	4.1 ± 2.8	0.0	1.0 ± 1.0	-
Vaccinium uliginosum	6.5 ± 1.9	12.9 ± 4.7	10.2 ± 4.0	2.7 ± 1.0	-
Graminoids					
Calamagrostis lapponica	0.0	0.0	6.1 ± 5.0	0.0	-
Carex vaginata	4.1 ± 0.9	9.5 ± 7.6	0.0	5.1 ± 3.2	-
Festuca ovina	0.0	0.0	0.0	2.4 ± 2.0	-
Poa alpigena	0.7 ± 0.4	2.4 ± 2.4	42.5 ± 8.8	0.3 ± 0.3	-
Forbs					
Astragalus alpinus	3.7 ± 1.9	1.0 ± 1.0	0.0	4.4 ± 3.6	-
Astragalus frigidus	1.4 ± 1.4	1.4 ± 1.4	0.0	0.0	-
Bartsia alpina	2.7 ± 2.7	0.0	0.0	0.0	-
Pedicularis lapponica	0.7 ± 0.7	0.0	0.0	0.0	-
Polygonum viviparum	2.0 ± 1.7	0.0	4.8 ± 3.4	3.1 ± 2.0	-
Pyrola rotundifolia	0.3 ± 0.3	0.0	0.0	0.0	-
Silena acaulis	0.0	0.0	0.0	2.0 ± 1.7	-
Tofieldia pusilla	0.7 ± 0.7	0.0	0.0	0.0	-
Thalictrum alpinum	0.0	0.0	0.0	2.4 ± 2.4	-
Vascular cryptograms					
Equisetum scirpoides	11.2 ± 4.7	8.8 ± 4.4	3.1 ± 1.1	5.1 ± 3.5	-
Mosses					
Aulacomnium turgidum	0.3 ± 0.3	1.4 ± 1.4	0.0	0.3 ± 0.3	-
Dicranum fuscescens	0.3 ± 0.3	0.0	0.0	2.4 ± 1.5	-

TABLE 4 (Continued)

	C	W	F	S	p-Value T
Hylocomium splendens	20.1±7.0	5.1±3.3	0.0	2.4±0.6	-
Paludella squarrosa	0.7±0.7	0.0	0.0	1.7±1.1	-
Tomentypnum nitens	1.0±0.5	2.0±2.0	0.0	1.0±0.7	-
Other moss	0.3±0.3	0.0	0.0	2.4±2.0	-
Lichens					
Peltigera aphtosa	0.7±0.4	0.3±0.3	0.0	0.0	-
Cladonia sp.	1.4±0.7	0.0	0.0	0.3±0.3	-
Cetraria nivalis	0.7±0.4	0.0	0.0	2.0±1.3	-
Other lichen	1.7±1.1	0.7±0.7	0.0	2.0±1.3	-

Note: p-Values from linear mixed-model (LMM) for main effects of treatment (T) on plant species functional groups are shown and p<.05 emboldened. Treatments not sharing a superscript letter within a plant species functional group differ significantly from each other (p<.05, LMM with Bonferroni test). "-" indicates variables (individual plant species) not tested with LMM.
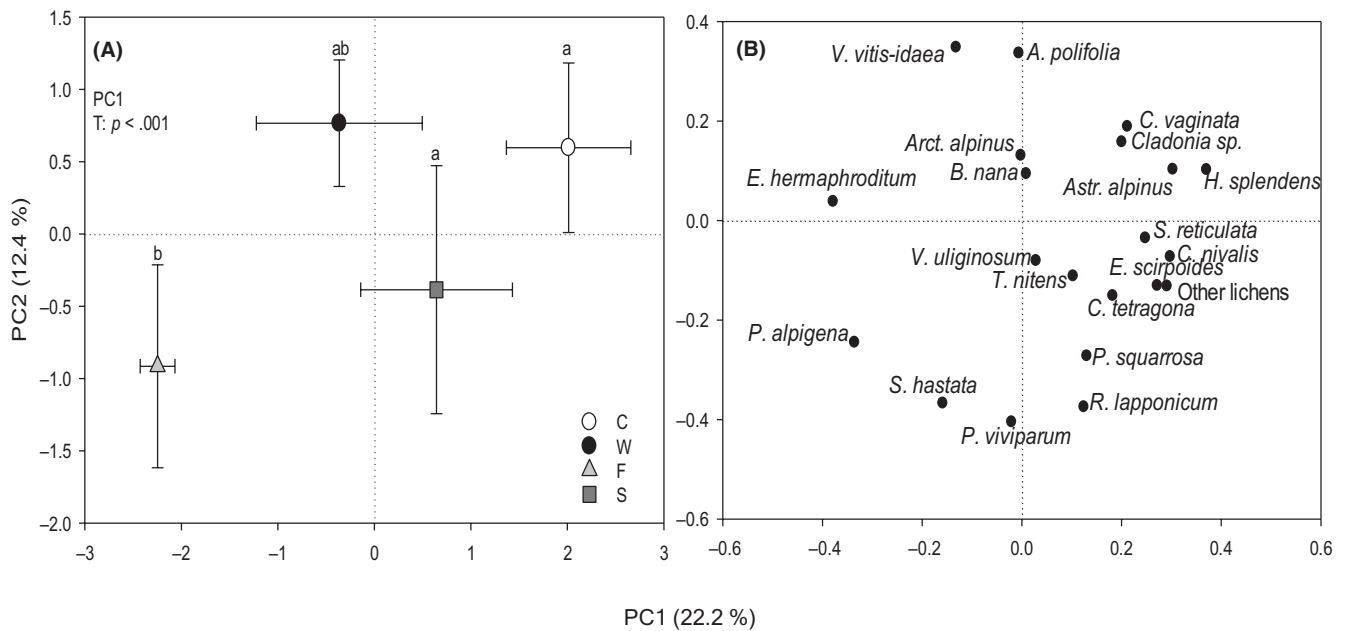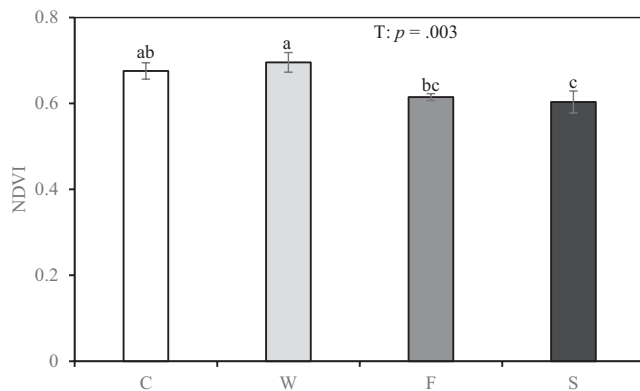

FIGURE 4 (A) The principal component (PC1 and PC2) scores (means±SEs, n=6) and (B) their corresponding loading variables for percentage cover of individual plant species. The variation explained by each PC is shown in parentheses. C, control; F, fertilization; S, shading; W, warming. The linear mixed-model (LMM) p-value for main effect of treatment (T) is shown in the figure. Treatments not sharing a letter differ significantly from each other (p<.05, LMM with Bonferroni test).

5 cm depths were not significant when the measurements were conducted. This suggests that the increased CO_2 emission from warmed and fertilized plots is primarily a result of long-term effects of warming and nutrient addition on soil properties and plant performance. There are previous reports of increased microbial biomass and activity and altered microbial community composition towards increased soil fungal or bacterial growth with warming and/or nutrient addition at the studied site (Hicks et al., 2020; Rinnan et al., 2007, 2013). For example, after 15 and 18 years of the treatment manipulations, microbial phospholipid fatty a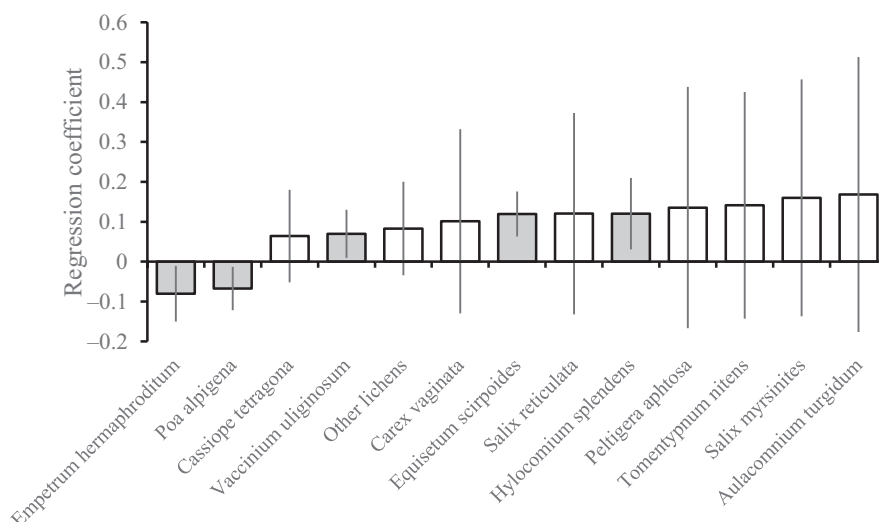cid (PLFA) concentration in the fertilized soils had increased by 16% and 31%, respectively (Rinnan et al., 2007). After 18 years of warming, microbial PLFAs were 20% higher in the warmed soils (Rinnan et al., 2013) and after 28 years of fertilization, the bacterial growth rate were also higher in the fertilized soils (Hicks et al., 2020).

At the studied experimental site, higher plant productivity in response to the long-term warming and fertilization treatments have also been well-documented (Campioli et al., 2012; Graglia et al., 2001; Hicks et al., 2020; Illeris et al., 2004; Jonasson et al., 1999; Michelsen et al., 2012; Ravn et al., 2017; Sorensen et al., 2012). For example,

in the recent assessments, after 22 years of the treatment manipulations, shrub height and vascular plant cover were significantly higher in the warmed and fertilized plots (Campioli et al., 2012; Sorensen et al., 2012) while there were also significant increases in shrub stem diameter and fine root biomass in the fertilized plots (Campioli et al., 2012; Ravn et al., 2017). After 26 years of the treatment manipulations, plant productivity had increased fourfold in the fertilized plots compared to the controls (Hicks et al., 2020). We also found evidence of higher plant productivity with increased nutrient availability after more than three decades of the treatment manipulations, as the cover of graminoids and total vascular plants were significantly higher in the fertilized treatments compared to the other treatments. The previous studies carried out at the same site suggested that the microbial responses to long-term warming and fertilization are likely driven by enhanced substrate inputs due to the stimulated plant productivity and may have manifested over time (Hicks et al., 2020; Ravn et al., 2017; Rinnan et al., 2013), resulting in increased ER rates through increased aboveground respiration and/or priming of soil organic matter decomposition and mineralization (Hicks et al., 2020; Ravn et al., 2017).

Furthermore, we observed significant increase in leaf litter inputs in the warmed and fertilized plots potentially due to stimulated plant productivity. These increased substrate inputs from additional plant material and root exudates may enhance microbial activity resulting in accelerated decomposition of soil organic matter and higher CO_2 release (Pedersen et al., 2017; Ravn et al., 2017; Rinnan et al., 2008). The increased litter production may also have a drying effect on the soil, especially in the fertilized plots where the soil moisture was significantly lower than the control, facilitating increased decomposition and heterotrophic respiration (Natali et al., 2015; Pedersen et al., 2017). Evidence of a decrease in C cycling in terms of decreased ER and photosynthesis due to shading has been observed at the same site in the early phase of the experiment (Christensen et al., 1997; Illeris et al., 2004). In this study, we found lower ER in the shaded plots, indicating lower C turnover rates, compared to the warmed and fertilized plots, in consistence with trends towards lower temperature and lower plant productivity in shaded plots (Campioli et al., 2012). The shading treatment also had lower ER than the control especially when the data was aggregated across measurement campaigns although the effects were not significant. Evidence of a decrease in nutrient cycling and productivity in the shaded plots was also observed in terms of a decrease in the vegetation greenness (NDVI) compared to the control and warmed plots.

FIGURE 5 Normalized differential vegetation index (NDVI) in control (C), warming (W), fertilization (F) and shading (S) plots/treatments. *p* Value for main effect of treatment (T) from linear mixed-model (LMM) is shown. Treatments not sharing a letter differ significantly from each other ($p < .05$, LMM with Bonferroni test).

4.2 | Methane fluxes

The maximum CH_4 uptake rates were comparable to, or lower than, earlier flux measurements at the site (Christensen et al., 1997) and fluxes reported in previous in situ studies carried out in similar arctic environments (Christiansen et al., 2014; Emmerton et al., 2014; Jørgensen et al., 2015). Methane fluxes were primarily negative, rendering the site a net CH_4 sink under all treatment conditions. The

FIGURE 6 Regression coefficients from Partial least square regression models on isoprene emissions in control, warming, fertilization, and shading plots/treatments. Error bars show ±2 standard deviations of the regression coefficients. Significant variables are marked with grey bars. Model is significant (CV-ANOVA) at $p < .05$.

functioning of this upland site as a net CH_4 sink could be attributed to the well-drained nature of the soils (Ravn et al., 2017), offering suitable conditions for methanotrophy (D'Imperio et al., 2023; Emmerton et al., 2014; Jørgensen et al., 2015; Whalen & Reeburgh, 1990). In line with our expectations, warming enhanced CH_4 sink strength of the ecosystem. Against our expectations, the shading treatment also enhanced CH_4 sink strength with no significant effects of the fertilization treatments.

Soil temperature and moisture are important factors controlling methanotrophy (D'Imperio et al., 2017; Emmerton et al., 2014; Jørgensen et al., 2015; Tate, 2015; Voigt et al., 2023). The soil temperature and moisture content could be influenced by the treatment manipulations and could act as temporal drivers of CH_4 uptake through their control on oxygen availability, C substrate availability, and presence, distribution, and activity of methanotrophs, as well as gas diffusion through soils (D'Imperio et al., 2017; Jørgensen et al., 2015; Voigt et al., 2023). In the current study, the impact of soil temperature and moisture as temporal drivers of CH_4 uptake was small or insignificant since the soil temperature and moisture in the warmed and shaded plots did not differ significantly from the control during measurements. Hence, the enhanced CH_4 uptake under warming and shading could be attributed to long term rather than temporal effects of these treatments on soil properties, such as soil moisture and substrate availability, affecting methanotrophy. At the same site, Rinnan et al. (2007) found that the warming and shading plots reduced the gravimetric soil water content after 15 years of treatment manipulation. Hence, the warming and shading treatments may have lowered the soil moisture content over time, enhancing methanotrophic activity by facilitating gas (CH_4 and O_2) diffusion into zones of active CH_4 oxidation in the warmed and shaded soils. In addition, increased CH_4 uptake may partly be linked to the increased ER rates in the warmed plots whereby input of plant-derived labile C, from root exudates and organic matter or litter decomposition, may serve as additional and alternative C source for methanotrophs, stimulating their growth and activity (Voigt et al., 2023).

Contrary to our hypothesis, nutrient addition had no effect on CH_4 uptake by the ecosystem. There exist contradictory results about the effects of N addition on soil CH_4 sink (Wu et al., 2022). Ammonium (NH_4^+) or N addition generally inhibits CH_4 oxidation in natural upland soils (Saari et al., 2004; Wu et al., 2022). However, other studies report no inhibition (e.g., Wu et al., 2022, and references there in) or even stimulation (e.g., Christensen et al., 1997) of CH_4 oxidation in response to addition of N. In this study, the nutrient addition have enhanced plant growth and biomass resulting to lower soil moisture in the fertilized plots, due to increased transpiration from the higher plant biomass. The drier soils favor CH_4 uptake by the ecosystem (Voigt et al., 2023) while the added nutrient (NH_4^+) is known inhibitor of CH_4 oxidation (Saari et al., 2004). These opposing responses to nutrient addition could produce a counterbalancing effect resulting to no change in CH_4 uptake as was observed in this study.

4.3 | Nitrous oxide fluxes

The rates of N_2O fluxes were in the range of fluxes measured in previous in situ studies carried out in similar arctic environments including a dry and moist lowland tundra (Chen et al., 2014), upland tundra, and vegetated peat surfaces (Marushchak et al., 2011; Repo et al., 2009; Voigt, Lamprecht, et al., 2017; Voigt, Marushchak, et al., 2017). Previous studies have reported low N_2O emissions from vegetated soils due to limited availability of mineral N (Marushchak et al., 2011; Repo et al., 2009; Voigt, Marushchak, et al., 2017). However, over time, increased temperatures may induce N_2O emissions from vegetated tundra surfaces by enhancing mineral N availability for microbial nitrification and denitrification to an extent greater than plant N uptake and microbial N immobilization (Voigt, Lamprecht, et al., 2017). Here, we show in situ evidence for the production and release of N_2O from vegetated tundra surfaces as a consequence of more than 30 years of warming, indicating that the warming treatments have enhanced mineral N availability over time leading to increased N_2O emissions. Hicks et al. (2020) reported a tendency towards higher gross N mineralization rates and unchanged concentrations of mineral N in fertilized plots after 26 years of nutrient addition at the same site. Here, after more than 30 years of nutrient addition, we found significant increase in N_2O emissions in the fertilized plots suggesting that the increased nutrient availability may have enhanced decomposition and N mineralization over time leading to increased availability of mineral N for microbial production and release of N_2O. Alternatively, the added nutrient and available mineral N may have been rapidly lost from the system through denitrification (Hicks et al., 2020) and as a consequence higher N_2O emissions in the fertilized plots. The higher N_2O emissions in the fertilized plots compared to the shaded plots indicates an increase in N-cycling resulting from enhanced plant productivity, litter inputs, substrate availability, and microbial activity under increased nutrient availability compared to the shaded conditions where reduced light availability may have limited plant productivity and C and N turnover rates.

4.4 | BVOC fluxes

Total BVOC emission rates in control plots averaged across all measurement campaigns were lower than those measured in situ in a high arctic tundra (Kramshøj et al., 2016), but were comparable to, or higher than, other in situ measurements carried out at a nearby wet heath (Tiiva et al., 2008; Valolahti et al., 2015). As hypothesized, warming increased the emissions of isoprene. Against our hypothesis, the emissions of the other BVOC groups were not affected by any of the treatments. When integrated over a growing season, the warming treatment causes an average air temperature increment of 3.5°C compared to the control, whereas the shading treatment decreased the average air temperature by 0.4°C compared to the control (Rieksta et al., 2021).

However, in the current study, the chamber enclosure temperatures in the warming and shading treatments did not differ significantly from the controls during the BVOC measurements in each campaign and when averaged across campaigns. Hence, the effect of warming on isoprene emissions was likely a consequence of a change in vegetation cover (i.e., higher plant biomass) and composition due to long-term warming (Valolahti et al., 2015) rather than as a result of direct biosynthetic stimulation of isoprene production by warming (Kramshøj et al., 2016; Seco et al., 2022; Tiiva et al., 2008). The emission profile of BVOCs is influenced by the coexistence of different plant species (Faubert et al., 2012). Isoprene emissions in the heath were positively associated with the cover of *V. uliginosum*, *E. scirpoides*, and *H. splendens*. The most likely reason was that these species grew in association with typical isoprene emitting plant species, such as *Carex* sp. and *Salix* spp. (Tiiva et al., 2008; Vedel-Petersen et al., 2015), present in the ecosystem and supported by the positive correlation between *E. scirpoides* and *S. reticulata*, and *H. splendens* and *C. vaginata*.

4.5 | Implications and future directions

Overall, long-term moderate temperature increase, and enhanced nutrient availability increased CO_2 emissions from the tundra heath. The release of CO_2 from (sub)arctic soils due to warming and increased nutrient availability is known to be substantial and persistent (Maes et al., 2024; Ravn et al., 2017) and should be of concern considering that CO_2 is a GHG with positive climate feedback effects. The long-term increase in plant productivity with a concurrent increase in ER due to warming and enhanced nutrient availability, based on this study and previous studies at the site (Hicks et al., 2020; Michelsen et al., 2012; Ravn et al., 2017), imply that (sub)arctic tundra ecosystems may be transformed from sinks to sources of CO_2 if the increase in ER were to exceed plant CO_2 uptake (Maes et al., 2024). Growing evidence suggests that (sub)arctic soils may also be relevant sources of N_2O (Marushchak et al., 2011; Repo et al., 2009; Voigt, Lamprecht, et al., 2017; Voigt, Marushchak, et al., 2017). Here, we present the first in situ evidence of N_2O emissions in response to climate change related manipulations of warming and increased nutrient availability at the study site. Since N_2O is a potent GHG with 273 times stronger warming potential than CO_2 in a 100 years' time horizon (IPCC, 2021), increased N_2O release will further enhance the radiative forcing emanating from C gases due to increased temperature and nutrient availability. Long-term moderate temperature increase, and shading (simulating increased cloudiness) enhanced CH_4 uptake and we suggest that decreased soil moisture and enhanced substrate availability played a role. Our observation of CH_4 uptake in all treatments supports previous studies suggesting that arctic and subarctic upland heath ecosystems constitute a significant sink for atmospheric CH_4 (Christensen et al., 1997; Voigt et al., 2023), which may be

enhanced under future conditions of increased temperature and increased cloudiness, providing negative feedback to climate.

Based on this study, changes in vegetation composition and biomass induced by long-term warming will indirectly increase isoprene emission from subarctic heath ecosystems (Tang et al., 2023) as well as reduce the C sink strength (via loss of C as isoprene) of these ecosystems. Meanwhile, the high potential of these ecosystems to function as CH_4 sinks may reduce the negative effect of isoprene on the atmospheric lifetime of CH_4 under future warming. The study emphasizes that climate warming and related environmental changes, such as increased nutrient availability and increased cloudiness, can have long lasting consequences for the C and N cycling and ecosystem-atmosphere exchange of trace gases in the Subarctic regions with important climate feedback implications. The current work reports for the effects of warming, increased nutrient availability, and increased cloudiness separately, although in the course of climate change, these factors will act in concert and may offset climate and ecosystem processes triggering important feedback loops. Hence, discriminating for the individual and combined effects of the different climate change factors represents the next step in unravelling the effects of climate change on ecosystem-atmosphere exchange of trace gases in the high latitudes.

AUTHOR CONTRIBUTIONS

Flobert A. Ndah: Conceptualization; formal analysis; funding acquisition; investigation; methodology; visualization; writing – original draft; writing – review and editing. **Anders Michelsen:** Conceptualization; investigation; methodology; resources; supervision; writing – review and editing. **Riikka Rinnan:** Conceptualization; methodology; resources; writing – review and editing. **Marja Maljanen:** Conceptualization; funding acquisition; methodology; resources; supervision; writing – review and editing. **Santtu Mikkonen:** Formal analysis; methodology; writing – review and editing. **Minna Kivimäenpää:** Conceptualization; formal analysis; funding acquisition; methodology; supervision; writing – review and editing.

CONFLICT OF INTEREST STATEMENT
The authors declare no conflicts of interest.

DATA AVAILABILITY STATEMENT
The data that support the findings of this study are openly available in figshare at https://doi.org/10.6084/m9.figshare.25674405.

ORCID

Flobert A. Ndah https://orcid.org/0000-0001-5504-8931
Anders Michelsen https://orcid.org/0000-0002-9541-8658
Riikka Rinnan https://orcid.org/0000-0001-7222-700X
Marja Maljanen https://orcid.org/0000-0002-7454-0064
Santtu Mikkonen https://orcid.org/0000-0003-0595-0657
Minna Kivimäenpää https://orcid.org/0000-0003-0500-445X

REFERENCES

Abisko Scientific Research Station. (2022). *Meteorological data June 1–September 30, 2022, temperature and precipitation data 1991–2020, Abisko Scientific Research Station, Polarforskningssekretariatet.* http://www.polar.se/abisko

Ball, B. A., Virginia, R. A., Barrett, J. E., Parsons, A. N., & Wall, D. H. (2009). Interactions between physical and biotic factors influence CO_2 flux in Antarctic dry valley soils. *Soil Biology and Biochemistry*, 41, 1510–1517. https://doi.org/10.1016/j.soilbio.2009.04.011

Bates, K. H., & Jacob, D. J. (2019). A new model mechanism for atmospheric oxidation of isoprene: Global effects on oxidants, nitrogen oxides, organic products, and secondary organic aerosol. *Atmospheric Chemistry and Physics*, 19, 9613–9640. https://doi.org/10.5194/acp-19-9613-2019

Boy, M., Zhou, P., Kurtén, T., Chen, D., Xavier, C., Clusius, P., Roldin, P., Baykara, M., Pichelstorfer, L., Foreback, B., Bäck, J., Petäjä, T., Makkonen, R., Kerminen, V. M., Pihlatie, M., Aalto, J., & Kulmala, M. (2022). Positive feedback mechanism between biogenic volatile organic compounds and the methane lifetime in future climates. *Climate and Atmospheric Science*, 5, 72. https://doi.org/10.1038/s41612-022-00292-0

Butterbach-Bahl, K., Baggs, E. M., Dannenmann, M., Kiese, R., & Zechmeister-Boltenstern, S. (2013). Nitrous oxide emissions from soils: How well do we understand the processes and their controls? *Philosophical Transactions of the Royal Society: Biological Sciences*, 368, 20130122. https://doi.org/10.1098/rstb.2013.0122

Campioli, M., Leblans, N., & Michelsen, A. (2012). Twenty-two years of warming, fertilisation and shading of subarctic heath shrubs promote secondary growth and plasticity but not primary growth. *PLoS One*, 7, e34842. https://doi.org/10.1371/journal.pone.0034842

Chen, Q., Zhu, R., Wang, Q., & Xu, H. (2014). Methane and nitrous oxide fluxes from four tundra ecotopes in Ny-Ålesund of the High Arctic. *Journal of Environmental Sciences*, 26(7), 1403–1410. https://doi.org/10.1016/j.jes.2014.05.005

Christensen, T. R., Michelsen, A., Jonasson, S., & Schmidt, I. K. (1997). Carbon dioxide and methane exchange of a subarctic heath in response to climate change related environmental manipulations. *Oikos*, 79(1), 34–44. https://doi.org/10.2307/3546087

Christiansen, J. R., Romero, A. J. B., Jørgensen, N. O. G., Glaring, M. A., Jørgensen, C. J., Berg, L. K., & Elberling, B. (2014). Methane fluxes and the functional groups of methanotrophs and methanogens in a young Arctic landscape on Disko Island, West Greenland. *Biogeochemistry*, 122, 15–33. https://doi.org/10.1007/s10533-014-0026-7

D'Imperio, L., Li, B.-B., Tiedje, J. M., Oh, Y., Christiansen, J. R., Kepfer-Rojas, S., Westergaard-Nielsen, A., Brandt, K. K., Holm, P. E., Wang, P., Ambus, P., & Elberling, B. (2023). Spatial controls of methane uptake in upland soils across climatic and geological regions in Greenland. *Communications Earth & Environment*, 4, 461. https://doi.org/10.1038/s43247-023-01143-3

D'Imperio, L., Nielsen, C. S., Westergaard-Nielsen, A., Michelsen, A., & Elberling, B. (2017). Methane oxidation in contrasting dry soil types: Responses to warming with implication for landscape-integrated CH_4 budget. *Global Change Biology*, 23(2), 966–976. https://doi.org/10.1111/gcb.13400

Elberling, B., Tamstorf, M. P., Michelsen, A., Arndal, M. F., Sigsgaard, C., Illeris, L., Bay, C., Hansen, B. U., Christensen, T. R., Hansen, E. S., Jakobsen, B. H., & Beyens, L. (2008). Soil and plant community-characteristics and dynamics at Zackenberg. *Advances in Ecological Research*, 40, 223–248. https://doi.org/10.1016/S0065-2504(07)00010-4

Ellebjerg, S. M., Tamstorf, M. P., Illeris, L., Michelsen, A., & Hansen, B. U. (2008). Inter-annual variability and controls of plant phenology and productivity at zackenberg. *Advances in Ecological Research*, 40, 249–273. https://doi.org/10.1016/S0065-2504(07)00011-6

Elmendorf, S., Henry, G., Hollister, R., Björk, R. G., Boulanger-Lapointe, N., Cooper, E. J., Cornelissen, J. H. C., Day, T. A., Dorrepaal, E., Elumeeva, T. G., Gill, M., Gould, W. A., Harte, J., Hik, D. S., Hofgaard, A., Johnson, D. R., Johnstone, J. F., Jónsdóttir, I. S., Jorgenson, J. C., ... Wipf, S. (2012). Plot-scale evidence of tundra vegetation change and links to recent summer warming. *Nature Climate Change*, 2, 453–457. https://doi.org/10.1038/nclimate1465

Emmerton, C. A., Louis, V. L. S., Lehnherr, I., Humphreys, E. R., Rydz, E., & Kosolofski, H. R. (2014). The net exchange of methane with high Arctic landscapes during the summer growing season. *Biogeosciences*, 11, 3095–3106. https://doi.org/10.5194/bg-11-3095-2014

Eriksson, L., Trygg, J., & Wold, S. (2008). CV-ANOVA for significance testing of PLS and OPLS® models. *Journal of Chemometrics*, 22, 594–600. https://doi.org/10.1002/cem.1187

Faubert, P., Tiiva, P., Michelsen, A., Rinnan, Å., Ro-Poulsen, H., & Rinnan, R. (2012). The shift in plant species composition in a Subarctic mountain birch forest floor due to climate change would modify the biogenic volatile organic compound emission profile. *Plant and Soil*, 352, 199–215. https://doi.org/10.1007/s11104-011-0989-2

Faubert, P., Tiiva, P., Rinnan, Å., Michelsen, A., Holopainen, J. K., & Rinnan, R. (2010). Doubled volatile organic compound emissions from Subarctic tundra under simulated climate warming. *New Phytologist*, 187(1), 199–208. https://doi.org/10.1111/j.1469-8137.2010.03270.x

Frolking, S., & Roulet, N. T. (2007). Holocene radiative forcing impact of northern peatland carbon accumulation and methane emissions. *Global Change Biology*, 13, 1–10. https://doi.org/10.1111/j.1365-2486.2007.01339.x

Gil, J., Marushchak, M. E., Rütting, T., Baggs, E. M., Pérez, T., Novakovskiy, A., Trubnikova, T., Kaverin, D., Martikainen, P. J., & Biasi, C. (2022). Sources of nitrous oxide and the fate of mineral nitrogen in subarctic permafrost peat soils. *Biogeosciences*, 19, 2683–2698. https://doi.org/10.5194/bg-19-2683-2022

Graglia, E., Jonasson, S., Michelsen, A., Schmidt, I. K., Havström, M., & Gustavsson, L. (2001). Effects of environmental perturbations on abundance of subarctic plants after three, seven and ten years of treatments. *Ecography*, 24, 5–12. https://doi.org/10.1034/j.1600-0587.2001.240102.x

Guenther, A. B., Hewitt, C. N., Erickson, D., Fall, R., Geron, C., Graedel, T., Harley, P., Klinger, L., Lerdau, M., Mckay, W. A., Pierce, T., Scholes, B., Steinbrecher, R., Tallamraju, R., Taylor, J., & Zimmerman, P. (1995). A global model of natural volatile organic compound emissions. *Journal of Geophysical Research*, 100, 8873–8892. https://doi.org/10.1029/94JD02950

Guenther, A. B., Zimmerman, P. R., Harley, P. C., Monson, R. K., & Fall, R. (1993). Isoprene and monoterpene emission rate variability: Model evaluations and sensitivity analyses. *Journal of Geophysical Research: Atmospheres*, 98, 12609–12617. https://doi.org/10.1029/93JD00527

Havström, M., Callaghan, T. V., & Jonasson, S. (1993). Differential growth responses of *Cassiope tetragona*, an arctic dwarf-shrub, to environmental perturbations among three contrasting high- and subarctic sites. *Oikos*, 66(3), 389–402. https://doi.org/10.2307/3544933

Hicks, L. C., Rousk, K., Rinnan, R., & Rousk, J. (2020). Soil microbial responses to 28 years of nutrient fertilization in a subarctic heath. *Ecosystems*, 23, 1107–1119. https://doi.org/10.1007/s10021-019-00458-7

Hiltbrunner, D., Zimmermann, S., Karbin, S., Hagedorn, F., & Niklaus, P. A. (2012). Increasing soil methane sink along a 120-year afforestation chronosequence is driven by soil moisture. *Global Change Biology*, 18, 3664–3671. https://doi.org/10.1111/j.1365-2486.2012.02798.x

Hobbie, S. E. (1996). Temperature and plant species control over litter decomposition in Alaskan tundra. *Ecological Monographs*, 66, 503–522. https://doi.org/10.2307/2963492

Hobbie, S. E., Nadelhoffer, K. J., & Högberg, P. A. (2002). A synthesis: The role of nutrients as constraints on carbon balances in boreal and arctic regions. *Plant and Soil*, 242, 163–170. https://doi.org/10.1023/A:1019670731128

Illeris, L., König, S. M., Grogan, P., Jonasson, S., Michelsen, A., & Ro-Poulsen, H. (2004). Growing-season carbon dioxide flux in a dry Subarctic heath: Responses to long-term manipulations. *Arctic, Antarctic, and Alpine Research*, 36, 456–463. https://doi.org/10.1657/1523-0430(2004)036[0456:GCDFIA]2.0.CO;2

IPCC. (2021). Climate change 2021: The physical science basis. In V. Masson-Delmotte, P. Zhai, A. Pirani, S. L. Connors, C. Péan, S. Berger, N. Caud, Y. Chen, L. Goldfarb, M. I. Gomis, M. Huang, K. Leitzell, E. Lonnoy, J. B. R. Matthews, T. K. Maycock, T. Waterfield, O. Yelekçi, R. Yu, & B. Zhou (Eds.), *Contribution of working group I to the sixth assessment report of the intergovernmental panel on climate change*. Cambridge University Press. https://doi.org/10.1017/9781009157896

Jonasson, S. (1988). Evaluation of the point intercept method for estimation of plant biomasses. *Oikos*, 52, 101–106. https://doi.org/10.2307/3565988

Jonasson, S., Michelsen, A., Schmidt, I. K., & Nielsen, E. V. (1999). Responses in microbes and plants to changed temperature, nutrient, and light regimes in the arctic. *Ecology*, 80, 1828–1843. https://doi.org/10.2307/176661

Jørgensen, C. J., Johansen, K. M., Westergaard-Nielsen, A., & Elberling, B. (2015). Net regional methane sink in high Arctic soils of northeast Greenland. *Nature Geoscience*, 8, 20–23. https://doi.org/10.1038/ngeo2305

Kecorius, S., Vogl, T., Paasonen, P., Lampilahti, J., Rothenberg, D., Wex, H., Zeppenfeld, S., van Pinxteren, M., Hartmann, M., Henning, S., Gong, X., Welti, A., Kulmala, M., Stratmann, F., Herrmann, H., & Wiedensohler, A. (2019). New particle formation and its effect on cloud condensation nuclei abundance in the summer Arctic: A case study in the Fram Strait and Barents Sea. *Atmospheric Chemistry and Physics*, 19, 14339–14364. https://doi.org/10.5194/acp-19-14339-2019

Kejna, M., Uscka-Kowalkowska, J., & Kejna, P. (2021). The influence of cloudiness and atmospheric circulation on radiation balance and its components. *Theoretical and Applied Climatology*, 144, 823–838. https://doi.org/10.1007/s00704-021-03570-8

Kramshøj, M., Albers, C. N., Svendsen, S. H., Björkman, M. P., Lindwall, F., Björk, R. G., & Rinnan, R. (2019). Volatile emissions from thawing permafrost soils are influenced by meltwater drainage conditions. *Global Change Biology*, 25, 1704–1716. https://doi.org/10.1111/gcb.14582

Kramshøj, M., Vedel-Petersen, I., Schollert, M., Rinnan, Å., Nymand, J., Ro-Poulsen, H., & Rinnan, R. (2016). Large increases in Arctic biogenic volatile emissions are a direct effect of warming. *Nature Geoscience*, 9, 349–352. https://doi.org/10.1038/ngeo2692

Kulmala, M., Nieminen, T., Nikandrova, A., Lehtipalo, K., Manninen, H. E., Kajos, M. K., Kolari, P., Lauri, A., Petaja, T., Krejci, R., Hansson, H.-C., Swietlicki, E., Lindroth, A., Christensen, T., Arneth, A., Hari, P., Back, J., Vesala, T., & Kerminen, V.-M. (2014). CO_2-induced terrestrial climate feedback mechanism: From carbon sink to aerosol source and back. *Boreal Environment Research: An International Interdisciplinary Journal*, 19, 122–131.

Laothawornkitkul, J., Taylor, J. E., Paul, N. D., & Hewitt, C. N. (2009). Biogenic volatile organic compounds in the Earth system. *The New Phytologist*, 183, 27–51. https://doi.org/10.1111/j.1469-8137.2009.02859.x

Li, T., Baggesen, N., Seco, R., & Rinnan, R. (2023). Seasonal and diel patterns of BVOC fluxes in a Subarctic tundra. *Atmospheric Environment*, 292, 119430. https://doi.org/10.1016/j.atmosenv.2022.119430

Liu, Y., Key, J. R., Liu, Z., Wang, X., & Vavrus, S. J. (2012). A cloudier Arctic expected with diminishing sea ice. *Geophysical Research Letters*, 39, L05705. https://doi.org/10.1029/2012GL051251

Loreto, F., & Schnitzler, J. P. (2010). Abiotic stresses and induced BVOCs. *Trends in Plant Science*, 15(3), 154–166. https://doi.org/10.1016/j.tplants.2009.12.006

Mack, M. C., Schuur, E. A. G., Bret-Harte, M. S., Shaver, G. R., & Chapin, F. S., III. (2004). Ecosystem carbon storage in arctic tundra reduced by long-term nutrient fertilization. *Nature*, 431, 440–443. https://doi.org/10.1038/nature02887

Maes, S. L., Dietrich, J., Midolo, G., Schwieger, S., Kummu, M., Vandvik, V., Aerts, R., Althuizen, I. H. J., Biasi, C., Björk, R. G., Böhner, H., Carbognani, M., Chiari, G., Christiansen, C. T., Clemmensen, K. E., Cooper, E. J., Cornelissen, J. H. C., Elberling, B., Faubert, P., ... Dorrepaal, E. (2024). Environmental drivers of increased ecosystem respiration in a warming tundra. *Nature*, 629, 105–113. https://doi.org/10.1038/s41586-024-07274-7

Magnani, M., Baneschi, I., Giamberini, M., Raco, B., & Provenzale, A. (2022). Microscale drivers of summer CO_2 fluxes in the Svalbard High Arctic tundra. *Scientific Reports*, 12, 763. https://doi.org/10.1038/s41598-021-04728-0

Marushchak, M. E., Pitkämäki, A., Koponen, H., Biasi, C., Seppälä, M., & Martikainen, P. J. (2011). Hot spots for nitrous oxide emissions found in different types of permafrost peatlands. *Global Change Biology*, 17, 2601–2614. https://doi.org/10.1111/j.1365-2486.2011.02442.x

Mastepanov, M., Sigsgaard, C., Tagesson, T., Ström, L., Tamstorf, M. P., Lund, M., & Christensen, T. R. (2013). Revisiting factors controlling methane emissions from high-Arctic tundra. *Biogeosciences*, 10, 5139–5158. https://doi.org/10.5194/bg-10-5139-2013

McGuire, A. D., Anderson, L. G., Christensen, T. R., Dallimore, S., Guo, L., Hayes, D. J., Heimann, M., Lorenson, T. D., Macdonald, R. W., & Roulet, N. (2009). Sensitivity of the carbon cycle in the Arctic to climate change. *Ecological Monographs*, 79, 523–555. https://doi.org/10.1890/08-2025.1

Michelsen, A., Rinnan, R., & Jonasson, S. (2012). Two decades of experimental manipulations of heaths and forest understory in the Subarctic. *Ambio*, 41, 218–230. https://doi.org/10.1007/s13280-012-0303-4

Natali, S. M., Schuur, E. A. G., Mauritz, M., Schade, J. D., Celis, G., Crummer, K. G., Johnston, C., Krapek, J., Pegoraro, E., Salmon, V. G., & Webb, E. E. (2015). Permafrost thaw and soil moisture driving CO_2 and CH_4 release from upland tundra. *Journal of Geophysical Research—Biogeosciences*, 120, 525–537. https://doi.org/10.1002/2014JG002872

Norris, J., Allen, R., Evan, A., Zelinka, M. D., O'Dell, C. W., & Klein, S. A. (2016). Evidence for climate change in the satellite cloud record. *Nature*, 536, 72–75. https://doi.org/10.1038/nature18273

Ortega, J., & Helmig, D. (2008). Approaches for quantifying reactive and low-volatility biogenic organic compound emissions by vegetation enclosure techniques—Part A. *Chemosphere*, 72(3), 343–364. https://doi.org/10.1016/j.chemosphere.2007.11.020

Pedersen, E. P., Elberling, B., & Michelsen, A. (2017). Seasonal variations in methane fluxes in response to summer warming and leaf litter addition in a Subarctic heath ecosystem. *Journal of Geophysical Research: Biogeosciences*, 122, 2137–2153. https://doi.org/10.1002/2017JG003782

Quintanilla Casas, B., Bro, R., Hinrich, J., & Davie-Martin, C. (2023). *Tutorial on PARADISe: PARAFAC2-based deconvolution and*

identification system for processing GC–MS data. https://doi.org/10.21203/rs.3.pex-2143/v1

Rantanen, M., Karpechko, A. Y., Lipponen, A., Nordling, K., Hyvärinen, O., Ruosteenoja, K., Vihma, T., & Laaksonen, A. (2022). The Arctic has warmed nearly four times faster than the globe since 1979. *Communications Earth & Environment*, *3*, 1–10. https://doi.org/10.1038/s43247-022-00498-3

Ravn, N. R., Ambus, P., & Michelsen, A. (2017). Impact of decade-long warming, nutrient addition and shading on emission and carbon isotopic composition of CO_2 from two Subarctic dwarf shrub heaths. *Soil Biology and Biochemistry*, *111*, 15–24. https://doi.org/10.1016/j.soilbio.2017.03.016

Repo, M. E., Susiluoto, S., Lind, S. E., Jokinen, S., Elsakov, V., Biasi, C., Virtanen, T., & Martikainen, P. J. (2009). Large N_2O emissions from cryoturbated peat soil in tundra. *Nature Geoscience*, *2*, 189–192. https://doi.org/10.1038/ngeo434

Rieksta, J., Li, T., Michelsen, A., & Rinnan, R. (2021). Synergistic effects of insect herbivory and changing climate on plant volatile emissions in the subarctic tundra. *Global Change Biology*, *27*, 5030–5042. https://doi.org/10.1111/gcb.15773

Rinnan, R., Michelsen, A., & Bååth, E. (2013). Fungi benefit from two decades of increased nutrient availability in tundra heath soil. *PLoS One*, *8*, e56532. https://doi.org/10.1371/journal.pone.0056532

Rinnan, R., Michelsen, A., Bååth, E., & Jonasson, S. (2007). Fifteen years of climate change manipulations alter soil microbial communities in a Subarctic heath ecosystem. *Global Change Biology*, *13*(1), 28–39. https://doi.org/10.1111/j.1365-2486.2006.01263.x

Rinnan, R., Michelsen, A., & Jonasson, S. (2008). Effects of litter addition and warming on soil carbon, nutrient pools, and microbial communities in a subarctic heath ecosystem. *Applied Soil Ecology*, *39*, 271–281. https://doi.org/10.1016/j.apsoil.2007.12.014

Ruess, L., Michelsen, A., Schmidt, I. K., & Jonasson, S. (1999). Simulated climate change affecting microorganisms, nematode density and biodiversity in subarctic soils. *Plant and Soil*, *212*, 63–73. https://doi.org/10.1023/A:1004567816355

Rustad, L., Campbell, J., Marion, G., Norby, R., Mitchell, M., Hartley, A., Cornelissen, J., Gurevitch, J., & GCTE-NEWS. (2001). A meta-analysis of the response of soil respiration, net nitrogen mineralization, and aboveground plant growth to experimental ecosystem warming. *Oecologia*, *126*, 543–562. https://doi.org/10.1007/s004420000544

Saari, A., Rinnan, R., & Martikainen, P. J. (2004). Methane oxidation in boreal forest soils: Kinetics and sensitivity to pH and ammonium. *Soil Biology and Biochemistry*, *36*(7), 1037–1046. https://doi.org/10.1016/j.soilbio.2004.01.018

Schuur, E. A. G., Bockheim, J., Canadell, J. G., Euskirchen, E., Field, C. B., Goryachkin, S. V., Hagemann, S., Kuhry, P., Lafleur, P. M., Lee, H., Mazhitova, G., Nelson, F. E., Rinke, A., Romanovsky, V. E., Shiklomanov, N., Tarnocai, C., Venevsky, S., Vogel, J. G., & Zimov, S. A. (2008). Vulnerability of permafrost carbon to climate change: Implications for the global carbon cycle. *Bioscience*, *58*, 701–714. https://doi.org/10.1641/B580807

Seco, R., Holst, T., Davie-Martin, C. L., Simin, T., Guenther, A., Pirk, N., Rinne, J., & Rinnan, R. (2022). Strong isoprene emission response to temperature in tundra ecosystems. *Proceedings of the National Academy of Sciences of the United States of America*, *119*(38), e2118014119. https://doi.org/10.1073/pnas.2118014119

Shupe, M. D., & Intrieri, J. M. (2004). Cloud radiative forcing of the Arctic surface: The influence of cloud properties, surface albedo, and solar zenith angle. *Journal of Climate*, *17*(3), 616–628. https://doi.org/10.1175/1520-0442(2004)017<0616:crfota>2.0.co;2

Siljanen, H. M., Welti, N., Voigt, C., Heiskanen, J., Biasi, C., & Martikainen, P. J. (2020). Atmospheric impact of nitrous oxide uptake by boreal forest soils can be comparable to that of methane uptake. *Plant and Soil*, *454*, 121–138. https://doi.org/10.1007/s11104-020-04638-6

Simin, T., Tang, J., Holst, T., & Rinnan, R. (2021). Volatile organic compound emission in tundra shrubs—Dependence on species

characteristics and the near-surface environment. *Environmental and Experimental Botany*, *184*, 104387. https://doi.org/10.1016/j.envexpbot.2021.104387

Smith, K. A., Dobbie, K. E., Ball, B. C., Bakken, L. R., Sitaula, B. K., Hansen, S., Brumme, R., Borken, W., Christensen, S., Priemé, A., Fowler, D., Macdonald, J. A., Skiba, U., Klemedtsson, L., Kasimir-Klemedtsson, A., Degórska, A., & Orlanski, P. (2000). Oxidation of atmospheric methane in Northern European soils, comparison with other ecosystems, and uncertainties in the global terrestrial sink. *Global Change Biology*, *6*, 791–803. https://doi.org/10.1046/j.1365-2486.2000.00356.x

Sorensen, P. L., Lett, S., & Michelsen, A. (2012). Moss specific changes in nitrogen fixation following two decades of warming, shading and fertilizer addition. *Plant Ecology*, *213*, 695–706. https://doi.org/10.1007/s11258-012-0034-4

Tang, J., Zhou, P., Miller, P. A., Schurgers, G., Gustafson, A., Makkonen, R., Fu, Y. H., & Rinnan, R. (2023). High-latitude vegetation changes will determine future plant volatile impacts on atmospheric organic aerosols. *npj Climate and Atmospheric Science*, *6*, 147. https://doi.org/10.1038/s41612-023-00463-7

Tate, K. R. (2015). Soil methane oxidation and land-use change—From process to mitigation. *Soil Biology and Biochemistry*, *80*, 260–272. https://doi.org/10.1016/j.soilbio.2014.10.010

Tholl, D., Boland, W., Hansel, A., Loreto, F., Röse, U. S. R., & Schnitzler, J.-P. (2006). Practical approaches to plant volatile analysis. *The Plant Journal*, *45*, 540–560. https://doi.org/10.1111/j.1365-313X.2005.02612.x

Tiiva, P., Faubert, P., Michelsen, A., Holopainen, T., Holopainen, J. K., & Rinnan, R. (2008). Climatic warming increases isoprene emission from a Subarctic heath. *New Phytologist*, *180*(4), 853–863. https://doi.org/10.1111/j.1469-8137.2008.02587.x

Topp, E., & Pattey, E. (1997). Soils as sources and sinks for atmospheric methane. *Canadian Journal of Soil Science*, *77*, 167–178. https://doi.org/10.4141/S96-107

Trumbore, S. (2006). Carbon respired by terrestrial ecosystems—Recent progress and challenges. *Global Change Biology*, *12*, 141–153. https://doi.org/10.1111/j.1365-2486.2006.01067.x

Valolahti, H., Kivimäenpää, M., Faubert, P., Michelsen, A., & Rinnan, R. (2015). Climate change-induced vegetation change as a driver of increased Subarctic biogenic volatile organic compound emissions. *Global Change Biology*, *21*(9), 3478–3488. https://doi.org/10.1111/gcb.12953

Vedel-Petersen, I., Schollert, M., Nymand, J., & Rinnan, R. (2015). Volatile organic compound emission profiles of four common arctic plants. *Atmospheric Environment*, *120*, 117–126. https://doi.org/10.1016/j.atmosenv.2015.08.082

Voigt, C., Lamprecht, R. E., Marushchak, M. E., Lind, S. E., Novakovskiy, A., Aurela, M., Martikainen, P. J., & Biasi, C. (2017). Warming of Subarctic tundra increases emissions of all three important greenhouse gases—Carbon dioxide, methane, and nitrous oxide. *Global Change Biology*, *23*, 3121–3138. https://doi.org/10.1111/gcb.13563

Voigt, C., Marushchak, M. E., Lamprecht, R. E., Jackowicz-Korczyński, M., Lindgren, A., Mastepanov, M., Granlund, L., Christensen, T. R., Tahvanainen, T., Martikainen, P. J., & Biasi, C. (2017). Increased nitrous oxide emissions from Arctic peatlands after permafrost thaw. *Proceedings of the National Academy of Sciences of the United States of America*, *114*, 6238–6243. https://doi.org/10.1073/PNAS.1702902114

Voigt, C., Virkkala, A. M., Hould Gosselin, G., Bennett, K. A., Black, T. A., Detto, M., Chevrier-Dion, C., Guggenberger, G., Hashmi, W., Kohl, L., Kou, D., Marquis, C., Marsh, P., Marushchak, M. E., Nesic, Z., Nykänen, H., Saarela, T., Sauheitl, L., Walker, B., … Sonnentag, O. (2023). Arctic soil methane sink increases with drier conditions and higher ecosystem respiration. *Nature Climate Change*, *13*, 1095–1104. https://doi.org/10.1038/s41558-023-01785-3

Wagner, I., Hung, J. K. Y., Neil, A., & Scott, N. A. (2019). Net greenhouse gas fluxes from three High Arctic plant communities along a

moisture gradient. *Arctic Science, 5*(4), 185–201. https://doi.org/10.1139/as-2018-0018

Whalen, S., & Reeburgh, W. (1990). Consumption of atmospheric methane by tundra soils. *Nature, 346*, 160–162. https://doi.org/10.1038/346160a0

Whalen, S. C. (2005). Biogeochemistry of methane exchange between natural wetlands and the atmosphere. *Environmental Engineering Science, 22*, 73–94. https://doi.org/10.1089/ees.2005.22.73

Wu, J., Cheng, X., Xing, W., & Liu, G. (2022). Soil-atmosphere exchange of CH$_4$ in response to nitrogen addition in diverse upland and wetland ecosystems: A meta-analysis. *Soil Biology and Biochemistry, 164*, 108467. https://doi.org/10.1016/j.soilbio.2021.108467

Zhang, Y., Zhang, N., Yin, J., Zhao, Y., Yang, F., Jiang, Z., Tao, J., Yan, X., Qiu, Y., Guo, H., & Hu, S. (2020). Simulated warming enhances the responses of microbial N transformations to reactive N input in a Tibetan alpine meadow. *Environment International, 141*, 105795. https://doi.org/10.1016/j.envint.2020.105795

SUPPORTING INFORMATION

Additional supporting information can be found online in the Supporting Information section at the end of this article.

How to cite this article: Ndah, F. A., Michelsen, A., Rinnan, R., Maljanen, M., Mikkonen, S., & Kivimäenpää, M. (2024). Impact of three decades of warming, increased nutrient availability, and increased cloudiness on the fluxes of greenhouse gases and biogenic volatile organic compounds in a subarctic tundra heath. *Global Change Biology, 30*, e17416. https://doi.org/10.1111/gcb.17416